Eur. Phys. J. D (2014) 68: 377
DOI: 10.1140/epjd/e2014-50717-x

THE EUROPEAN PHYSICAL JOURNAL D

Colloquium

Quantum optics with quantum dots

Towards semiconductor sources of quantum light for quantum information processing

Alexios Beveratos[1], Izo Abram[1], Jean-Michel Gérard[2], and Isabelle Robert-Philip[1,a]

[1] CNRS-Laboratoire de Photonique et de Nanostructures, Route de Nozay, 91460 Marcoussis, France
[2] CEA-CNRS-UJF, "Nanophysique et Semiconducteurs" group, CEA−INAC−SP2M, 38054 Grenoble, France

Received 29 September 2014 / Received in final form 4 November 2014
Published online 18 December 2014 –

Abstract. For the past fifteen years, single semiconductor quantum dots, often referred to as solid-state artificial atoms, have been at the forefront of various research direction lines for experimental quantum information science, in particular in the development of practical sources of quantum states of light. Here we review the research to date, on the tailoring of the emission properties from single quantum dots producing single photons, indistinguishable single photons and entangled photon pairs. Finally, the progress and future prospects for applications of single dots in quantum information processing is considered.

1 Introduction

Quantum information science aims at harnessing the distinctive features of quantum physics, especially superposition and entanglement, to enhance the functionality and power of information and communication technologies. It has been a thriving interdisciplinary field of research for the last thirty years, extending from the fundamental investigation of quantum phenomena to the experimental implementation of disruptive quantum-enabled technologies. In quantum information science, the information is encoded on a quantum bit (qubit) consisting of any two-level quantum system, its two states representing the digits 0 and 1. Among quantum systems, photons constitute a natural choice for communication and metrology, and a promising route for quantum simulation and computing. All these applications require ideally deterministic light sources that can deliver on demand single photons, indistinguishable single photons or entangled photon pairs, produced at high repetition rate. Several schemes have been established to produce such quantum states of light as for instance attenuated lasers (which suffer, however, from the Poissonian distribution of the emitted photons) or non-linear optics. Presently, most experiments in quantum optics or photonic quantum information processing rely on non-linear optical sources allowing the preparation of time-bin [1] or polarization [2] entangled photons as well as heralded single photons [3]. Although down-conversion sources are still primarily employed due the high purity of the emitted quantum states of light, such sources suffer in particular from the probabilistic generation of photons combined with a trade-off between the repetition rate and the probability of emitting multiple photon pairs simultaneously.

Another scheme for generating efficiently and deterministically single photon states on demand uses the emission of a single quantum emitter, such as an atom [4,5], an ion [6,7], a molecule [8,9] or a nitrogen-vacancy center in diamond [10,11]. An attractive alternative for an all solid-state single quantum system is that of a semiconductor quantum dot. In this paper we review the progress towards the realization of quantum dot-based sources for the generation of quantum states of light. In the following section, we recall the basic concepts related to the optical properties of semiconductor quantum dots. In the third section, we introduce the various approaches developed for efficiently producing single photons on demand, and then we present the different strategies implemented for restoring photon indistinguishability as well as different schemes for producing entangled photons out of single quantum dots. Finally, we discuss some of the prospects in this field.

2 Semiconductor quantum dots: a solid-state emitter with discrete energy levels

Quantum dots are semiconductor nanocrystals embedded in another semiconductor which presents a wider energy bandgap between its valence and conduction states. This results in a three dimensional potential well that confines the carriers (electrons and holes) in the nanocrystal, so that the electron and hole motion is quantized in all three spatial directions. This gives rise to discrete energy levels, each one accommodating up to two electrons or holes of

[a] e-mail: isabelle.robert@lpn.cnrs.fr

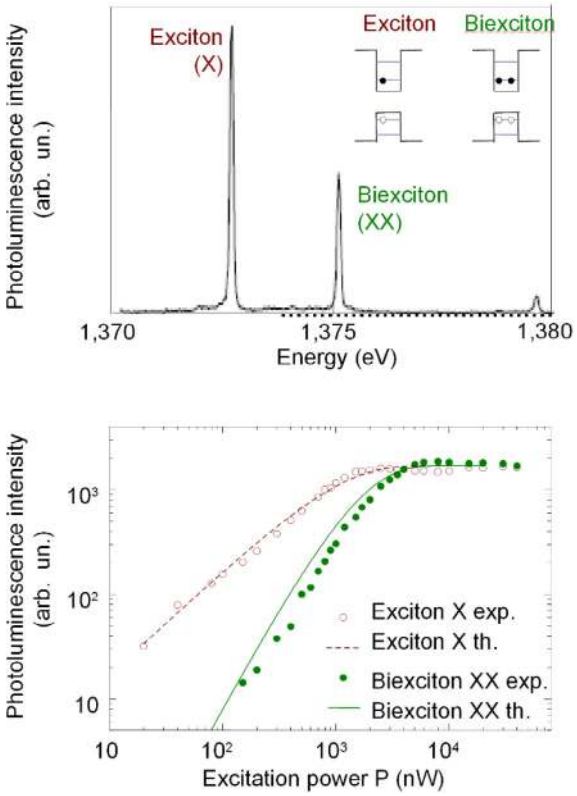

Fig. 1. (Top) Photoluminescence spectrum of a single InAs/GaAs quantum dot at 4 K under pulsed non-resonant optical excitation at energies higher than the GaAs bandgap; the incident power corresponds to 1.5 trapped electron-hole pairs in the dot on average. (Bottom) Dependance of the experimental integrated intensity of the exciton (red empty dots) and biexciton (green full dots) emission as a function of the pulsed excitation power. The lines correspond to the theoretical power dependance of the exciton (dash red line) and biexciton (solid green line) intensities, calculated by use of a simple rate-equation model.

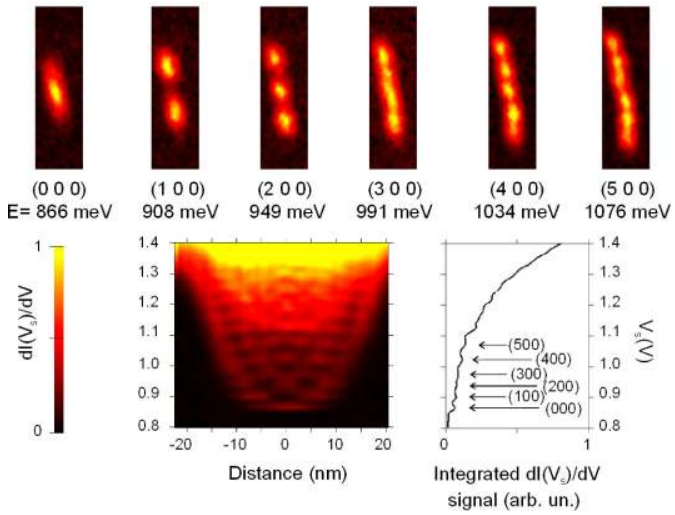

Fig. 2. (Top) Maps of the wavefunctions of the first five electronic levels in the conduction band of a single InAsP/InP quantum dot, measured by STM/STS. The lowest-energy map (top left) displays the expected elliptic intensity distribution for the (000) ground state corresponding to the *s*-shell, while the higher energy maps present lobe features with an increasing number of nodes along the (110) direction consistent with (n00) states. (Bottom) Differential conductivity, reflecting the local density of states, measured in a STS measurement as a function of the applied voltage and of the distance from the dot center along the base of the quantum dot; this measurement reveals the harmonicity of the dot's lateral potential. The differential conductance integrated along the dot base is also shown. All measurements were done at 4 K on a single InAsP/InP dot with apparent width and height of 42 and 5.9 nm, respectively. Experimental results reproduced from reference [23].

opposite spin as in the case of single atoms (see Figs. 1 and 2). For this reason, semiconductor quantum dots are often referred to as "artificial atoms", that is as a semiconductor analogue of single atoms.

One type of quantum dots can be formed by synthesizing nanometer-size core-and-shell structures by wet chemical approaches (colloidal quantum dots). Such dots have demonstrated their potential as single photon emitters [9,12,13], even at room temperature [14]. The control of growth kinetics in the wet chemical process also allows full control of the shape, resulting in dot-in-rods or in tetrapods as well as dot dimers or clusters in the same shell [15,16]. Embedding dots in a rod permits, in particular, control of the polarization of the emitted single photons [14].

Most experiments on quantum light generation from quantum dots, however, rely on another type of quantum dots, grown epitaxially, as these dots are particularly stable and display excellent optical properties, with no bleaching or blinking. They can emit under both electrical and optical pumping and can be easily integrated in optical microcavities. In this review, we shall focus more particularly on self-assembled InAs/GaAs quantum dots obtained in the Stranski-Krastanov self-organized growth mode [17–20]. Their growth is achieved by molecular beam epitaxy and exploits the small mismatch between the lattice constants of InAs and GaAs. When InAs is deposited on a GaAs substrate, it starts as a two-dimensional layer. When its thickness exceeds a certain critical value there is a transition into a three-dimensional growth mode, in order to relax the strain accumulated by the lattice mismatch. The resulting three-dimensional InAs nanostructures (i.e. the quantum dots), whose surface density can be as low as 10 μm^{-2}, are subsequently capped by GaAs material and lie on the remaining two-dimensional InAs layer, the so-called "wetting layer". The quantum dots are shaped like flat lenses of 3 nm in height and 20 nm in diameter on average, with large size variations among the dots within the same growth run. The exact size and material composition of a quantum dot determine its energy structure and emission wavelengths.

The electronic structure of a self-assembled quantum dot is composed of a few discrete energy levels in the conduction and valence bands, situated below the continuum

of states of the wetting layer. The lowest energy electron-hole states have a s-like envelope-wavefunction symmetry (hydrogen-like), while the next highest energy states have a p-like, d-like, ... symmetries. This discretization of the electronic levels in individual dots can be experimentally revealed by scanning tunneling microscopy and spectroscopy (STM/STS) [21–23]. Figure 2 presents maps of the wavefunctions of the dot's successive electronic (nmp) states in the conduction band, where the quantum numbers n, m and p correspond to the number of nodes in the (110), (1$\bar{1}$0) and (001) directions, respectively.

At low excitation power and temperature, illumination by a non-resonant laser creates electron-hole pairs in the GaAs substrate. These carriers efficiently relax towards the fundamental electron and hole levels of the quantum dot. As shown schematically on Figure 1, a quantum dot can thus trap one electron and one hole on the s-shell, forming an exciton, which may then recombine radiatively, producing a single photon. The dot can also capture two electrons and two holes with opposite spins on the s-shell (a "biexciton"), producing a cascade of two photons as the dot undergoes two successive transitions, from the biexciton to the exciton and then from the exciton to the ground state [24,25]. Importantly, the energies of these two photons differ slightly, due to the Coulomb interactions among the carriers in the dot, as can be seen on Figure 1 (top). Other emission lines can also exist, due to the multiplicity of the possible electronic excitations in the dot, such as charged excitons formed by an exciton with extra electrons or holes, charged biexcitons, multiexciton states formed by N electron-hole pairs, etc. with the corresponding optical transition energies all differing from the exciton and biexciton energies.

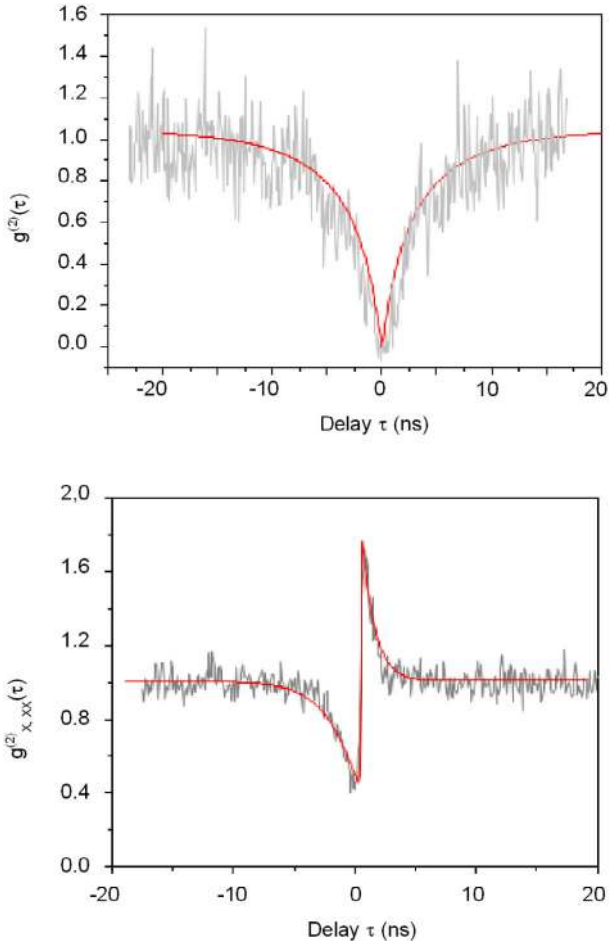

Fig. 3. (Top) Second-order correlation function measured on the exciton emission line of a single InAs/GaAs quantum dot, under continuous non-resonant optical pumping; the dot, cooled at 4 K, contains on average 0.06 exciton. (Bottom) Second-order cross-correlation function between the biexciton and the exciton emission lines of a single InAs/GaAs quantum dot, under continuous non-resonant optical pumping; the dot, cooled at 4 K, contains on average 0.2 exciton. Red lines show correlations expected from a simple rate equation model [29]. Experimental results reproduced from reference [24].

3 Producing single photons

3.1 Single photon generation under non-resonant excitation

When isolating and exciting non-resonantly a single quantum dot cooled to low temperature (typically 4 K), several electron-hole pairs are injected in the dot. These pairs recombine successively in a cascade process, ending with the one-exciton emission which can be exploited to produce single photons on demand [26]. At low excitation powers, only one or two pairs are captured in the dot, so that its emission spectrum is dominated by the exciton and biexciton lines (see Fig. 1 (top)). By spectrally filtering the exciton line, one single photon per excitation cycle is produced, provided the lifetime of the carrier reservoir (in particular of the wetting layer) is short compared with the radiative lifetime of the exciton. This scheme has been successfully implemented and studied experimentally through the second-order correlation function obtained in a Hanbury-Brown and Twiss set-up [27,28] (see Fig. 3 (top)): the spectrally-filtered emission from the exciton is sent to a 50/50 beamsplitter and the single photon nature of the exciton emission is evidenced by the absence of photodetection coincidences on the two output ports of the beamsplitter, since single photons can not split at a beamsplitter. This scheme can be extended to the generation of cascaded photons by spectrally filtering the biexciton and exciton emission lines [24,25,29,30]: The quantum dot produces a first photon at the biexciton energy and then a second photon at the exciton energy (see Fig. 3 (bottom)). The observed strong linear polarization of the two photons of the biexciton cascade [31,32] can be understood by considering the electron and hole spin structure in the quantum dot. The projection of the electron spin on the growth axis is either $1/2$ or $-1/2$, whereas the heavy-hole spin projection is either $3/2$ or $-3/2$. As a result, four distinct spin values exist for one exciton in the dot, among which two bright states with total spin of ± 1 that are coupled to the light field and are ideally degenerate. However, in practice, this degeneracy is lifted because

the dot is usually not fully symmetric, resulting in a doublet with a splitting in the range of 0−100 μeV as will be discussed in Section 5.2. As a consequence, the individual emission lines from the $|\pm 1\rangle$ states possess orthogonal linear polarization, typically aligned with the substrate cleavage directions ((110) and (1$\bar{1}$0) in the case of GaAs).

3.2 Single photon generation rate

The production of single photons on demand by a quantum dot is a necessary condition for quantum information processing, but is not sufficient since the collection of these single photons at a high rate presents many challenges.

The first one is related to the inherent mesoscopic nature of the quantum dot confinement, which can accommodate multiple electron-hole pairs. When increasing the excitation power, so as to increase the single photon generation rate, multiple electron-hole pairs are captured by the quantum dot, so that its luminescence spectrum, in addition to the sharp lines attributable to well-defined transitions (such as the exciton or the biexciton), includes also a broad but less-intense quasi-continuous background [33,34]. This background arises from the interaction of discrete carrier states associated to particles confined in the dot and a quasi-continuum associated to particles in the wetting layer, as well as from dephasing processes (discussed in Sect. 4) [35,36]. In this situation, spectral filtering of the exciton line cannot eliminate the part of the broad background lying in the vicinity and below the sharp line, thus degrading the deterministic single-photon character of the source, since the residual background corresponds to undesirable multiphoton pulses. Suppression of the background can be achieved either by non-resonant pumping at very low power (usually corresponding to a mean number of electron-hole pairs captured in the dot much lower than one per excitation cycle) or by resonant pumping, as discussed later on [37].

Another effect degrading the single-photon collection rate, arises from the low geometric efficiency of light collection. Quantum dots are embedded in a solid matrix, so that the emitted light is trapped in the material surrounding the dot, due to total internal reflection at the semiconductor-air interface. Various approaches have been proposed to improve the collection efficiency, based on modifying the geometry or on exploiting cavity quantum electrodynamics effects [38]. The narrow emission lines of single quantum dots at low temperature make them compatible with the exploitation of cavity quantum electrodynamics effects, in particular the Purcell effect, in which the exciton emission, when coupled to a low-loss and small-volume resonant cavity mode, is funneled predominantly into that mode [39]. By engineering the far-field emission diagram of the mode, the exciton emission can be efficiently collected by external optics. Implemented either on pillar microcavities [40,41] (see Fig. 4 (left)) or on photonic crystal cavities [42], the Purcell effect, associated to an optimized collection setup, has led to a detected single-photon flux as high as few tens MHz [43]. One challenge here is the resonant character of the Purcell effect,

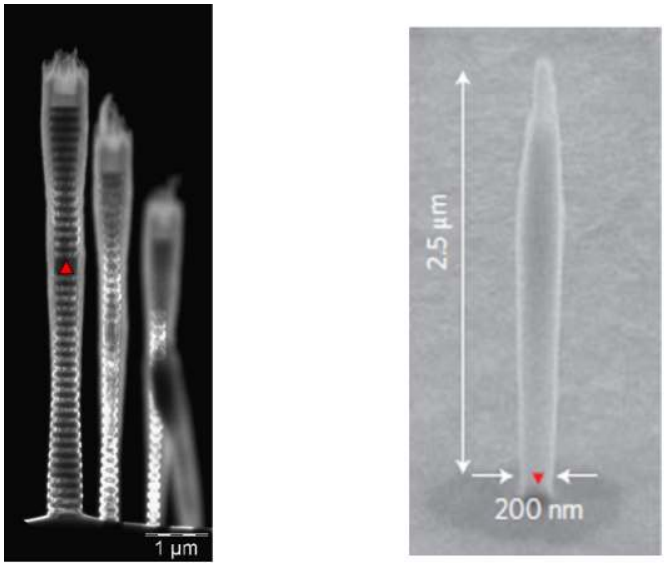

Fig. 4. (Left) Transmission electron microscopy image of a micropillar cavity confining light laterally via guiding effects and vertically via the presence of two Bragg mirrors. (Right) Scanning electron microscopy image of a wire with tapered end. These two geometries have been implemented to enhance the single photon collection efficiency. The dot position is schematically represented by red triangles.

requiring spatial and spectral overlap between the exciton and the cavity field. Spectral overlap can be achieved by tuning the exciton frequency through temperature adjustment [44], Stark shift [45], Zeeman shift [46] or strain tuning [47], while the cavity may be tuned into resonance through photorefractive effects [48] or gas condensation deposition [49]. Spatial overlap between the quantum dot and the cavity mode can be achieved by building the cavity around a quantum dot whose exact location is determined either during growth (discussed in Sect. 6) or post-growth via AFM or photoluminescence measurements [50,51]. The spectral matching constraint inherent in the cavity approach, may be relaxed by use of a spectrally broadband nanostructure such as a waveguide [52] or a nanowire antenna with a carefuly tapered end shaping the far-field radiation diagram [53–58] (see Fig. 4 (right)). This non-resonant approach can achieve up to 70% collection efficiency combined with a lower multiphoton emission probablity than the cavity approach [54]. The reason is that in nanowires, the proximity of the surface greatly reduces the carrier lifetime in the wetting layer, thus reducing the probability of recapture by the dot of a second electron-hole pair during the non-resonant pulsed excitation cycle. In both approaches, control of the mode polarization permits the generation of single photons in a well-defined polarization state [40,43,59].

3.3 Single photon generation under resonant excitation

While most experiments on single photon generation from quantum dots use a non-resonant optical excitation,

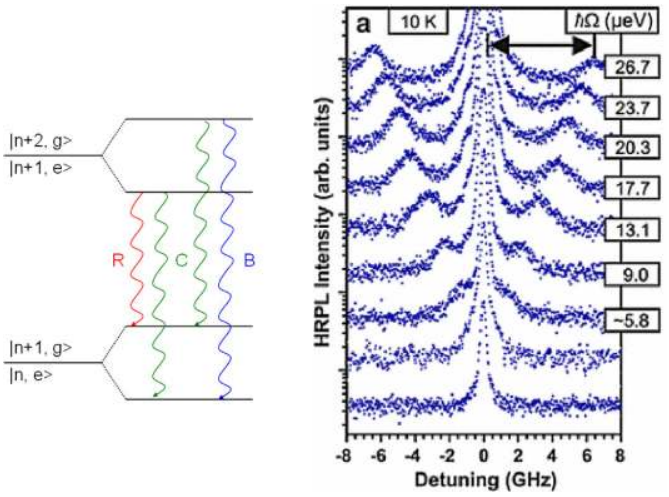

Fig. 5. (Left) Schematic representation of the dressed states between an exciton and a strong laser field. The optical transitions corresponding to the central (C) spectral line and the two sidebands at lower (R – Red-shifted line) and higher (B – Blue-shifted line) energies, are shown. (Right) Experimental spectra for increasing resonant laser powers observed on a single InAs/GaAs quantum dot, displaying three peaks corresponding to the Mollow triplet; the single dot is embedded in a Bragg micropillar cavity, suppressing light scattering normal to the pillar for laser light excitation orthogonal to the pillar axis. Experimental results reproduced from reference [63].

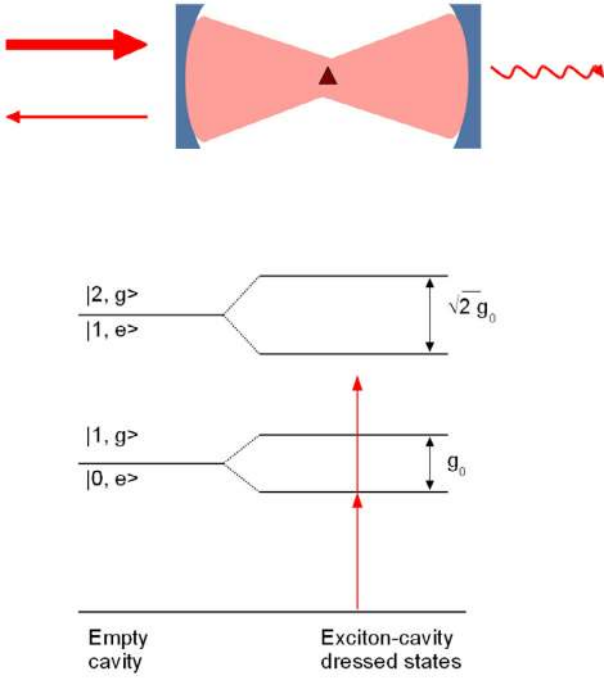

Fig. 6. Schematic description of the photon blockade effect in the strong coupling regime. The interaction between the exciton and the cavity mode produces non-equidistant energy levels, thus shiftin the cavity off-resonance as soon as one photon enters it.

resonant excitation into the excitonic state constitutes a promising alternative.

A two-level system excited on resonance by an intense continuous optical field produces a fluorescence spectrum composed of three distinct peaks, known as the Mollow triplet [60,61] (see Fig. 5 (right)). The emergence of these peaks can be explained in the dressed-state picture (see Fig. 5 (left)). In the absence of electromagnetic interaction, the state consisting of an excited two-level system and n photons resonant with it ($|e, n\rangle$) is degenerate with the state consisting of ground state of the two-level system and $n+1$ photons ($|g, n+1\rangle$). The electromagnetic interaction, however, lifts the degeneracy, leading to a ladder of dressed states schematically shown on Figure 5 (left). Four optical transitions are allowed along this ladder, two of them being degenerate, thus leading to a three-peaked fluorescence spectrum.

Experimental observation of the Mollow triplet requires strong discrimination of the scattered excitation laser light from the resonantly emitted single photons, by use of collection optics with strong spectral and polarization selectivity [62] or modal engineering of the dot's environment through its integration in a cavity allowing for orthogonal excitation and collection directions [63–65] (see Fig. 5 (right)). Concomitantly to the observation of the Mollow triplet, antibunching of the photons generated on the two sidebands (B and R on Fig. 5) has been demonstrated [66].

3.4 Photon blockade in the strong coupling regime

Most of the experiments involving coupling between a quantum dot and a cavity described up to now, were realized in the weak coupling regime, that is in the situation in which the strength of the electromagnetic coupling is smaller than all linewidths involved, so that the time-evolution of the exciton is essentially an irreversible exponential decay. In the strong coupling regime, on the other hand, the time scale of coherent coupling between the exciton and the cavity field is shorter than that of the decay into radiative and non-radiative channels. This results in a coherent periodic exchange of energy between the emitter and the field mode, the so-called vacuum Rabi oscillation, in striking contrast to the familiar irreversible exponential decay of the weak coupling regime. In the strong coupling regime, the interaction of the single emitter with a single mode of the cavity is described, as in the case of the Mollow triplet, by the Jaynes-Cummings Hamiltonian in which the system formed by the exciton and the light field is considered as a single system with a non-equidistant energy ladder (see Figs. 5 (left) and 6). For n photons in the cavity mode and a coupling constant g_0 between the exciton and the cavity field, the initially degenerate states $|e, n\rangle$ and $|g, n+1\rangle$ are mixed and split by $\sqrt{n}g_0$. The interaction thus causes the cavity to be shifted off resonance, so that presence of a first photon in the cavity prevents another photon from entering the cavity until the first photon leaves (see Fig. 6). This system thus allows filtering a coherent state into a train of

single photons, an effect known as a photon blockade. The resulting anti-bunched output has been observed experimentally for quantum dots isolated in photonic crystal cavities [67]. Photon bunching has also been observed by tuning the laser field in two-photon resonance with the eigenstates of the second Jaynes-Cummings manifold [68].

3.5 Towards practical devices for quantum key distribution

Beyond diminishing the rate of multiphoton pulses and increasing the single photon rate, two other issues have been addressed in view of implementing practical single photon sources.

One of them is electrical pumping. Most of experiments on quantum light generation by single dots rely on optical excitation. Yet, electrical pumping has also been made possible by embedding the dots in conventional *p-i-n* junctions [69], as well as in microcavity-enhanced light emitting diode-type structures increasing the single photon rate [70–72], in particular at telecommunications wavelengths [73,74].

The second issue is related to the single photon wavelength. For quantum key distribution protocols exploiting single photon states, it is desirable to operate in the two transmission windows of silica fibers around 1.3 μm and 1.55 μm. Most experiments, however, use InAs/GaAs dots producing single photons at wavelengths around 800 nm and up to 1 μm. In order to reach the fiber telecommunications spectral windows, one possibility is to use a different material system: InGaAs/InAs/GaAs dots can reach emission wavelengths around 1.3 μm [75–77], while InAsP/InP dots emit up to 1.55 μm [34,78–81]. Single photon emission from the exciton states has been evidenced in these two material systems, however still with significant multiphoton pulses. Another approach to reach the telecommunications bands, and more generally to implement tunable sources, consists of combining a quantum dot-based single photon source with a non-linear material (mainly periodically-poled lithium niobate waveguides) implementing wavelength conversion. Frequency up-conversion towards the visible spectrum [82] and down-conversion to telecommunications wavelengths [83,84] have been shown to preserve the quantum nature and coherence of the converted single photons [83,85]. A more challenging prospect would be to use the intrinsic non-linearity of the material surrounding the dot: an integrated approach involving a single quantum dot coupled to a non-linear optical resonator has been proposed in reference [86].

Non-linear processes can also alter the shape of the emitted single photons. The wavepacket of a single photon produced by a single dot presents an exponentially decaying tail. However Gaussian-shaped pulses are more favorable for some practical applications, such as interfacing with atomic quantum memories. Among the various techniques for reshaping single photon wavepackets [87–89], up-conversion processes have been exploited to convert a single photon with exponentially decaying profile to a single photon with a Gaussian profile and shorter duration [82].

4 Producing indistinguishable single photons

4.1 The issue of dephasing

Quantum information processing requires that the photons involved be indistinguishable, so that they behave as ideal Bosons. That is, they must have the same polarization and be in the same spectral-temporal as well as spatial mode, so that they are "identical" in every way.

In principle, a photon emitted by a quantum dot is a wavepacket of exponentially decaying time-profile with a characteristic time T_1, the lifetime of the emitting state and should correspond to a Lorentzian spectrum of width $1/T_1$. However, several physical processes in the quantum dot "mark" each photon differently while it is being emitted and thus compromise indistinguishability. These are collision-like brief, sudden and random changes of the exciton (or biexciton) energy, due to interactions with phonons or with a passing charged carrier, that interrupt the phase evolution of the electromagnetic oscillation and thus cause "dephasing", that is randomization of the phase of the electromagnetic wave corresponding to the photon. If these phase interruptions occur with a characteristic time T_2^* the photon wavepacket maintains its phase memory (and is thus indistinguishable from another wavepacket with the same initial phase) during a time T_2, given by $1/T_2 = 1/T_2^* + 1/2T_1$, while its spectrum is broadened to $1/T_2$ [90]. T_2 is usually called the "coherence decay time", while T_2^* is the pure dephasing time. Comparison of the radiative lifetime with the coherence time, obtained from the transition spectrum gives the degree of indistinguishability (given by $T_2/2T_1$) of two photons with the same temporal and spectral profiles. Complete indistinguishability requires that $T_2 = 2T_1$, so that the wavepacket temporal profile and frequency spectrum are Fourier transforms of each other.

While dephasing cannot be completely eliminated in the solid state, there are several ways of minimizing its impact. In general, the pure dephasing rate ($1/T_2^*$) increases with temperature and with the energy difference between the quantum dot exciton and the pumping laser, because both these situations increase the number of phonons present in the semiconductor and thus speed up dephasing [91,92]. Thus the simplest way to reduce the impact of dephasing is to reduce the number of phonons in the semiconductor by working at low temperature and/or by tuning the pump laser as close to resonance as possible. In addition, the radiative lifetime may be considerably shortened by use of a resonant cavity and the Purcell effect, so that it becomes dominant in determining the coherence time of the photons. Lastly, measurement of indistinguishability may be hindered by the presence of temporal jitter in the initiation of photon emission due to fluctuations in the time of formation of the exciton, for example if there is re-capture of an electron-hole pair from

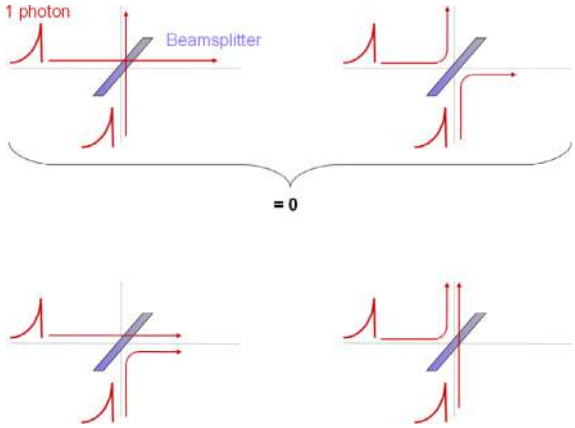

Fig. 7. Principle of two-photon interference in a Hong-Ou-Mandel experiment: Two indistinguishable photons are incident on the two input ports of a beamsplitter. These two photons can either be transmitted or reflected. However the probability amplitudes of the two configurations in which the two photons leave along two different output ports (both photons transmitted or both reflected), interfere destructively. Consequently the only outcome of the experiment corresponds to two photons emerging from the beamsplitter on the same output (one photon reflected and one photon transmitted), as if they had coalesced. This results in a suppression of simultaneous photodetection events on the two output ports.

the substrate or if the exciton state is reached following a radiative cascade from a multi-carrier state.

4.2 Restoring indistinguishability by cavity effects and quasi-resonant pumping

The first experiments for restoring indistinguishability relied on a combined reduction of the emission lifetime and increase of the pure dephasing time [93]. Reduction of the emission lifetime was achieved by use of the Purcell effect. Increase of the pure dephasing time was achieved by reducing the operating temperature down to 4 K and by implementing a quasi-resonant optical pumping of the dot, which reaches an excited state on the p-shell that relaxes to the exciton. This greatly reduces dephasing both because it generates few phonons and because it creates no multiple-carrier states, ensuring at the same time that no multi-photon pulses are emitted, as can be seen on Figure 8 (top).

The indistinguishability of photons emerging from a cavity containing a quantum dot can be studied by two-photon interference in a Hong-Ou-Mandel-type experiment, whose principle [94] is shown on Figure 7. When two indistinguishable photons are incident on the two input ports of a beamsplitter, they both leave the beamsplitter on the same output port. Two-photon interference of two single photons emitted successively by a quantum dot in a weakly coupled micropillar [93,95,96] or photonic crystal cavity [97], has demonstrated restoration of indistinguishability (measured by the depth of the two-photon interference dip) of up to 80% [93,98] (see Fig. 8 (bottom)).

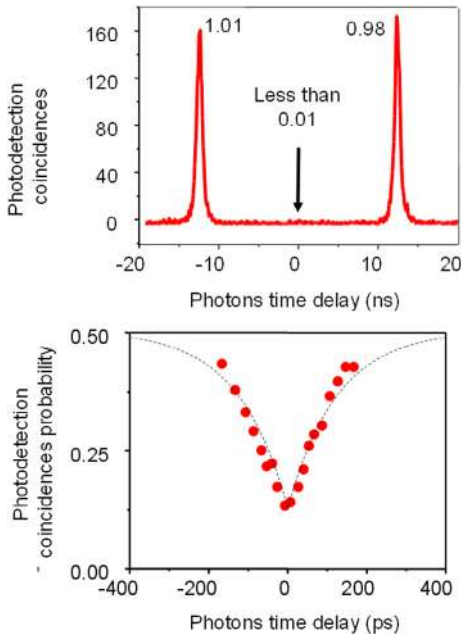

Fig. 8. (Top) Pulsed photodetection coincidences measured in a Hanbury-Brown and Twiss set-up on the exciton emission line of a single InAs/GaAs quantum dot. The normalized area of each peak is shown. (Bottom) Probability, in a Hong-Ou-Mandel experiment, that the two photons leave on different output ports of the beamsplitter, as a function of the time delay between the two photons. Red dots are experimental data while black line is deduced from a model fit. In these two experiments, the photons are produced by a single InAs/GaAs quantum dot, under quasi-resonant optical pumping; the dot, cooled at 4 K, is embedded in a micropillar cavity.

4.3 Restoring indistinguishability by resonant pumping

In the non-resonant and quasi-resonant approach, measurement of the degree of indistinguishability of the emitted photons is limited by temporal jitter and by dephasing. In order to increase the mutual coherence between the emitted photons, one solution relies on resonant pumping of the excitonic transition. Under these conditions, the time uncertainty in the emission process depends solely on the spontaneous decay, while dephasing is affected solely by phonon scattering since the contribution of carrier-carrier scattering is significantly minimized. However, the challenge here is the discrimination of the quantum dot resonance fluorescence signal from the residual scattered laser.

In the regime of strong resonant pump power, the emission spectrum consists of three lines, known as the Mollow triplet, as discussed in Sect. 2. In this regime, indistinguishable photons have been generated from single dots both under continuous-wave [63,99] and under excitation with resonant pulses that achieve full inversion of the exciton transition (π-pulses) [100,101]. Both experiments evidenced an improved mutual coherence between the emitted photons compared with quasi-resonant approaches, with two-photon interference visibility contrast

up to 97% (however at the cost of a poor collection efficiency limited to roughly 1%).

Under a low-intensity, resonant and continuous pump, the interaction of the electromagnetic field with the exciton system does not give rise to the Mollow sidebands and has a dominant coherent component, so that the scattered photons are free from dephasing. In this regime, the scattered photon spectrum replicates the excitation field and the scattered single photons inherit the coherence time of the excitation laser, as shown on single dots in [102,103]. The resulting spectrum is even narrower than the natural linewidth of the exciton (imposed by its radiative lifetime), allowing the generation of indistinguishable single photons whose coherence and indistinguishability are driven by the laser coherence time [104].

Indistinguishable photons have also been produced under non-resonant electrical pumping. For the case of electrically-pumped diodes producing single photons, an alternative technique has been developed whereby the excitonic transition is rapidly Stark-shifted during the emission process and photons are collected only when the transition is within a spectral window determined by an external filter, thus artificially reducing the observation time of the photon from T_1 to T_{filt}, the time during which the Stark-shifted frequency is within the filter bandwidth [105], however at the cost of a reduced collection rate.

5 Producing entangled photons

Quantum entanglement, one of the fundamental concepts embodying the "strangeness" of quantum mechanics, involves nonlocal correlations between distinct (and even distant) systems. It was first demonstrated in 1982 in an experiment based on Bell's inequality which sets the upper limit for the correlation between two classical (non-quantum) systems [106]. Since then, it has become an important element in the arsenal of quantum optics and has become an enabling resource of quantum information processing and communications technologies. Several schemes have been established to produce entangled photons, that are now routinely used in that context, using single atoms [106], non-linear processes [107,108] or single quantum dots.

5.1 Entangling indistinguishable single photons

The first experiment to produce entangled photons out of single quantum dots relied on post-selective linear-optics techniques to prepare two indistinguishable photons into a polarization-entangled state [109]. In this experiment (see Fig. 9 (top)), two sequential single photons are prepared in a linear polarization state and sent on the (non-polarized) input port of an unbalanced interferometer. The polarization of the photon traveling in the long arm of the interferometer is then rotated by 90 degrees, and the arm length difference is adjusted so that the two photons collide on the output mirror of the interferometer. It is then verified

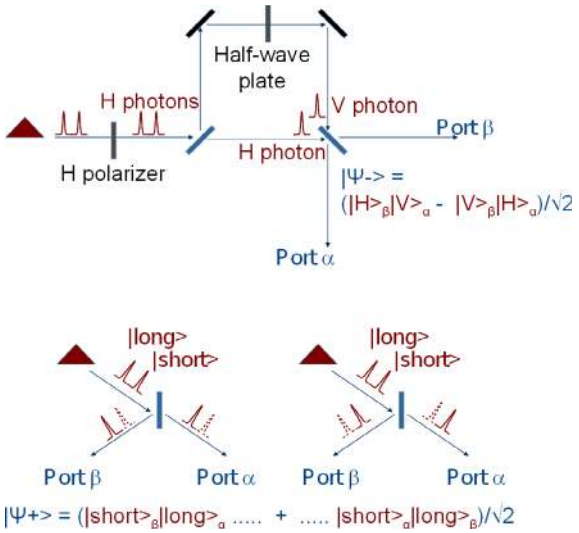

Fig. 9. (Top) Optical set-up to generate post-selected polarization entangled photons out of two sequential single photons. (Bottom) Optical set-up to generate post-selected time-bin entangled photons out of two sequential single photons: the two configurations in which the two photons leave on two different output ports of the beamsplitter, are indistinguishable in a Franson-type set-up, leading to time-position entanglement.

by post-selection that two photons emerging separately, along the two different output ports of the interferometer, are polarization entangled and violate Bell's inequality.

Another strategy exploits interference on a beamsplitter to produce post-selected time-bin entangled photons [110]. Two sequential indistinguishable single photons (denoted $|short\rangle$ and $|long\rangle$ on Fig. 9 (bottom)), are separated by a time delay long compared with the single photon pulse duration, and are incident on the same input port of a beamsplitter. If the configurations in which both photons follow the same output port (α or β) are discarded, the post-selected state, obtained with a probability 1/2 at the output of the beamsplitter, reads: $|\Psi_+\rangle = (|short\rangle_\alpha|long\rangle_\beta + |long\rangle_\alpha|short\rangle_\beta)/\sqrt{2}$. This state is a time-bin entangled state, that can be further analyzed in a Franson-type photon correlation set-up which uses two unbalanced interferometers so that the long-path photon catches up with the short-path photon [111,112]. Violation of Bell's inequality in such an experiment requires an "indistinguishability" ratio $T_2/2T_1$ higher the $1/\sqrt{2}$ [113]. This is within reach by use of single-dot based sources as shown in [114]: by use of a microcavity-enhanced quantum dot source operating under quasi-resonant pumping, time-bin entangled photons were produced in a Franson-type experiment.

5.2 Entangled photons out of the biexciton cascade

Entangled photons can also be produced out of the biexciton cascade. Generation of time-bin entangled photons has been proposed, based on the coherent creation of a photon pair starting from the biexciton level following preparation

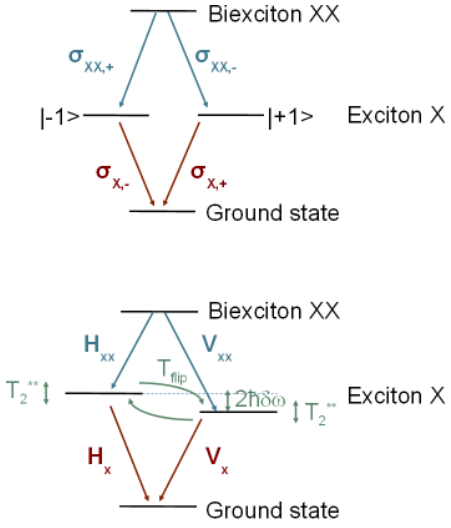

Fig. 10. Schematic description of the biexcitonic cascade in a typical quantum dot (top) with zero energy splitting on the relay excitonic level, leading to polarization maximally-entangled photons $(|\sigma_{XX+}, \sigma_{X-}\rangle + |\sigma_{XX-}\sigma_{X+}\rangle)/\sqrt{2}$ and (bottom) with an energy splitting $\hbar\delta\omega$ leading to two colinearly polarized photons in a single preferred basis. Relaxation mechanisms between the two excitonic relay levels (on a time scale T_{flip}) as well as cross-dephasing (on a time scale T_2^{**}) between the two excitonic states can also occur.

of the dot in a long-lived metastable state [115,116]. Recently, non-deterministic generation of time-bin entangled photons was achieved experimentally through two-photon resonant excitation of the biexciton [117].

Another scheme, which has been largely investigated, exploits the polarization properties of the photons produced from the biexciton state. The biexciton consists of two electron-hole pairs with opposite angular momenta trapped in the dot, and decays radiatively through two bright exciton relay states. In the first step of the cascade, a photon is emitted with random polarization. Conservation of angular momentum requires that the polarization of the photon emitted in the second step of the cascade be fixed relative to the first photon: the pair of photons is in a polarization-entangled state (see Fig. 10 (top)) [30]. First experiments on the polarization correlation of the two photons, revealed strong correlation along only one polarization basis [31,32], whereas entanglement requires correlation along all possible bases. The reason that no entanglement was observed is that it was possible to identify the relay exciton state. As discussed in Section 3, the exciton level in quantum dots is usually split by the anisotropic exchange interaction, caused by in-plane anisotropy of the exciton wave function (see Fig. 10 (bottom)). Measurement of the photon energy provides information on which pathway the two photon were released, thus destroying the quantum superposition that constitutes the entanglement.

Various strategies have been investigated to reduce the excitonic energy splitting to within the radiative linewidth of the relay levels: tuning of the splitting via application of in-plane magnetic fields [118], application of an in-plane [119,120] or out-of-plane [121] electric field, quantum dot annealing [122], control of the nanostructure growth [123] or strain tuning [124]. Some other strategies were proposed for compensating the impact of the fine structure splitting, in particular cavity effects [125,126] or strong spectral filtering [127]. Production of polarization-entangled photons has been demonstrated by use of a magnetic field and growth control [128], spectral filtering [127], out-of-plane electric field [129], optical Stark effect [130], quantum dot annealing [131] or strong temporal filtering [132]. In particular, temporal gating of the detection of the biexciton cascade (to eliminate spurious correlations with the background) has permitted observation of entanglement with violation of Bell's inequality of up to 4.5 standard deviations [133]. Entanglement out of dots embedded in a light-emitting-diode, has also been achieved [134].

Several other mechanisms may induce loss of entanglement [135]. In the solid-state environment, dephasing interactions that do not affect identically the two relay levels and whose impact depends on the polarization of the excitonic states, may degrade the strong correlations between the polarization of the two photons, even in the absence of splitting of the two exciton levels. Similarly, any incoherent mechanism inducing a population exchange between the excitonic levels (such as transitions through the dark states or spin-flip processes) deteriorates the visibility of entanglement. Various strategies for compensating these effects are possible as for example temporal filtering [132] (however discarding most of the photons produced) or cavity effects that may also favor the production rate of photon pairs [125]. However, when relying on cavity effects, various constraints have to be taken into account in order to avoid any which-path information degrading entanglement [136]: spatial mode indistinguishability of the two polarization modes (in terms of radiation diagram for instance), symmetric Purcell effect along the two polarization modes... Some cavities satisfy these constraints, such as plasmonic nanocavities [137], photonic crystal cavities [136] or double pillars [131].

In most of the above experiments, the photons produced are polarization-entangled but not necessarily indistinguishable. However, in advanced quantum information protocols, entanglement and indistinguishability are two key prerequisites. In order to restore the photon indistinguishability in polarization entangled-photon pairs, some strategies described in Section 4 have been exploited [138,139]. For instance, by implementing a resonant π-pulse excitation by two-photon absorption on the biexciton, indistinguishable and polarization-entangled photons have been produced out of the biexciton cascade [139].

6 Outlook

The progress during the last fifteen years in the development of quantum dot-based sources producing quantum states of light has opened the way to the realization

of a few building blocks for quantum information processing. One could mention quantum teleporation [140], quantum key distribution links [141–144], implementation of the Deutsch-Jozsa algorithm [145] or quantum logic gates [146,147]. In addition, the interfacing of the emitted single photons with an atomic vapor slow-light medium was achieved [148], an important step towards the storage of the quantum dot emission for the implementation of quantum memories and quantum repeaters. First steps towards the implementation of on-chip quantum circuits, including photon sources based on quantum dots, have also been demonstrated [149]. One of the advantages of quantum dot-based sources compared with non-linear sources is their deterministic and triggered nature which permits the production of heralded quantum states of light. However, the lower purity of the quantum states produced and the relative impractical handling of the source (resonant or quasi-resonant pumping, cryogenic operation, complex control of the emitted wavelength...) still hinder their systematic use. Although quantum dot-based sources delivering quantum states of light with either high purity or high efficiency have been demonstrated, deterministic sources combining both these qualities without multiphoton pulses and delivering entangled indistinguishable pairs of photons, are still lacking.

In order to engineer such sources, various directions are presently being prospected. In addition to the resonant or quasi-resonant schemes for enhancing purity and indistinguishability or engineering the single photons waveforms [150], one direction concerns the growth of wetting layer-free dots fabricated by the droplet epitaxy growth method [151]. Such dots display a better carrier confinement and high optical quality, even though the quantum efficiency demonstrated so far does not compete yet with Stranski-Krastanov dots [152]. The possibility of growing such dots on (111) substrates with C_{3v} symmetry, allows the growth of highly symmetric dots, with greatly reduced excitonic fine structure splitting. In addition to narrow linewidths [153], this approach has led to the demonstration of filtering-free violation of Bell's inequality for droplet epitaxial GaAs/AlGaAs dots [154]. More recently, a vanishing excitonic fine structure splitting at telecommunications wavelengths was observed in droplet epitaxial quantum dots [155].

The solid-state nature of quantum dot sources is conducive to scalability. One challenge here is going beyond the one or two quantum bit level to multi-qubit entangled states. However, the wide diversity of shapes and sizes of self-assembled quantum dots on the same growth substrate, represents a real bottleneck. One pioneering experiment in that direction involves two-photon interference between two spatially separate quantum dots [156,157]. In that experiment, quantum dot diversity was circumvented by selecting within the sample a few quantum dots that, by chance, presented similar optical properties, and then carrying out local in situ fine tuning. A more promising but still prospective approach is the growth of site-controlled quantum dots, for example by growing the dots in small apertures predesigned on the substrate by lithography. The first demonstration of single photon emission from such dots was obtained in the InGaAs/GaAs system emitting around 900 nm [158]. Site-controlled dots emitting indistinguishable single photons [159] or at telecommunications wavelengths [160], have also been demonstrated. Moreover, as for droplet epitaxy, one advantage here is the possibility to grow such dots on (111) substrates, making them good candidates for the generation of polarization-entangled photons as shown in [161]. Another approach is the growth of quantum dots in nanowires. Such dots are epitaxied using bottom-up growth (usually vapor-liquid-solid epitaxy catalyzed by gold nanoparticles), allowing for an unprecedented freedom of design in the axial as well as the lateral directions since strain is not the driving force for growth. Such versatility allows manipulation of both the electronic and optical properties of the epitaxied dots [162]. The wire geometry permits efficient light extraction for the implementation of efficient single photon sources with Gaussian emission pattern [59,163]. At the same time, their high symmetry makes them good candidates for efficiently producing entangled photons [164].

The possible use of single dots for quantum physics and quantum information science is not restricted to the generation of quantum states of light. Quantum dots may also find applications as spin qubits with long coherence times, of the order of the nanosecond, which can be lengthened to microseconds by optical spin echo techniques [165]. The electron or hole spin can be initialized [166,167] and manipulated [168,169] via optical approaches. Some presently pursued directions are the coupling of remote spins via a cavity mode or two-photon interference. First experiments in that direction include the optical control of the entanglement between two spins in two vertically stacked dots [170], entanglement between a quantum dot spin and a single photon [171], transfer of quantum information carried by a photon to the spin using quantum teleportation [172] or spin interfaces via connected photonic waveguides [173]. For more details on the spin properties of dots, we refer the reader to the two reviews of references [174,175].

7 Conclusion

In the past fifteen years, remarkable progress has been achieved in the understanding and use of the optical properties of single quantum dots. The present knowledge of these solid-state emitters is sufficiently mature to identify the promising direction lines, in which exploration of the potential of dots for quantum physics and information science, may be viable. The rich optical properties of single dots are now better understood, the ability to tailor the dot's emission has been demonstrated and efficient strategies to enhance the purity of the emitted quantum states of light have been implemented, establishing the basis for solid-state quantum information processing with quantum dots. The different pieces of the puzzle allowing for implementing highly efficient on-demand sources of quantum light with high purity from quantum dots, are gathered and may now be put together.

References

1. J. Brendel, W. Tittel, H. Zbinden, N. Gisin, Phys. Rev. Lett. **82**, 2594 (1999)
2. P.G. Kwiat, K. Mattle, H. Weinfurter, A. Zeilinger, A.V. Sergienko, Y. Shih, Phys. Rev. Lett. **75**, 4337 (1995)
3. S. Fasel, O. Alibart, S. Tanzilli, P. Baldi, A. Beveratos, N. Gisin, H. Zbinden, New J. Phys. **6**, 163 (2004)
4. H. Kimble, M. Dagenais, L. Mandel, Phys. Rev. Lett. **39**, 691 (1977)
5. P. Grangier, G. Roger, A. Aspect, Europhys. Lett. **1**, 173 (1986)
6. F. Dietrich, H. Walter, Phys. Rev. Lett. **58**, 203 (1987)
7. M. Keller, B. Lange, K. Hayasaka, W. Lange, H. Walther, Nature **431**, 1075 (2004)
8. T. Bashé, W.E. Moerner, M. Orrit, H. Talon, Phys. Rev. Lett. **69**, 1516 (1992)
9. B. Lounis, W.E. Moerner, Nature **407**, 491 (2000)
10. C. Kurtsiefer, S. Mayer, P. Zarda, H. Weinfurter, Phys. Rev. Lett. **85**, 290 (2000)
11. A. Beveratos, R. Brouri, T. Gacoin, J.-P. Poizat, P. Grangier, Phys. Rev. A **64**, 061802 (2001)
12. B. Lounis, H.A. Bechtel, D. Gerion, P. Alivisatos, W.E. Moerner, Chem. Phys. Lett. **329**, 399 (2000)
13. P. Michler, A. Kiraz, C. Becher, W.V. Schoenfeld, P.M. Petroff, L. Zhang, E. Hu, A. Imamoglu, Science **290**, 2282 (2000)
14. A. Qualtieri, G. Morello, P. Spinicelli, M.T. Todaro, T. Stomeo, L. Martiradonna, M. De Giorgi, X. Quélin, S. Buil, A. Bramati, J.P. Hermier, R. Cingolani, M. De Vittorio, New J. Phys. **11**, 033025 (2009)
15. J. Hu, L.S. Li, W. Yang, L. Manna, L.W. Wang, A.P. Alivisatos, Science **292**, 2060 (2001)
16. L. Manna, D.J. Milliron, A. Meisel, E.C. Scher, A.P. Alivisatos, Nat. Mater. **2**, 382 (2003)
17. L. Goldstein, F. Glas, J.Y. Marzin, M.N. Charasse, G. Le Roux, Appl. Phys. Lett. **47**, 1099 (1985)
18. D. Leonard, M. Krishnamurthy, C.M. Reaves, S.P. Denbaars, P.M. Petroff, Appl. Phys. Lett. **63**, 3203 (1993)
19. J.M. Moison, F. Houzay, F. Barthe, L. Leprince, E. André, O. Vatel, Appl. Phys. Lett. **64**, 196 (1994)
20. J.M. Gérard, J.B. Génin, J. Lefebvre, J.M. Moison, N. Lebouché, F. Barthe, J. Cryst. Growth **150**, 351 (1995)
21. B. Grandidier, Y.M. Niquet, B. Legrand, J.P. Nys, C. Priester, D. Stievenard, J.M. Gérard, V. Thierry-Mieg, Phys. Rev. Lett. **85**, 1068 (2000)
22. J.C. Girard, A. Lemaître, A. Miard, C. David, Z.-Z. Wang, J. Vac. Sci. Technol. B **27**, 891 (2009)
23. B. Fain, I. Robert-Philip, A. Beveratos, C. David, Z.-Z. Wang, I. Sagnes, J.-C. Girard, Phys. Rev. Lett. **108**, 126808 (2012)
24. E. Moreau, I. Robert-Philip, L. Ferlazzo, V. Thierry-Mieg, J.-M. Gerard, I. Abram, Phys. Rev. Lett. **87**, 183601 (2001)
25. D.V. Regelman, U. Mizrahi, D. Gershoni, E. Ehrenfreund, W.V. Schoenfeld, P.M. Petroff, Phys. Rev. Lett. **87**, 257401 (2001)
26. J.M. Gérard, B. Gayral, J. Lightwave Technol. **17**, 2089 (1999)
27. C. Santori, M. Pelton, G. Solomon, Y. Dale, Y. Yamamoto, Phys. Rev. Lett. **86**, 1502 (2001)
28. I. Robert, E. Moreau, J.-M. Gérard, I. Abram, J. Lumin. **94**, 797 (2001)
29. M.H. Baier, A. Malko, E. Pelucchi, D.Y. Oberli, E. Kapon, Phys. Rev. B **73**, 205321 (2006)
30. O. Benson, C. Santori, M. Pelton, Y. Yamamoto, Phys. Rev. Lett. **84**, 2513 (2000)
31. C. Santori, D. Fattal, M. Pelton, G.S. Solomon, Y. Yamamoto, Phys. Rev. B **66**, 045308 (2002)
32. R.M. Stevenson, R.M. Thompson, A.J. Shields, I. Farrer, B.E. Kardynal, D.A. Ritchie, M. Pepper, Phys. Rev. B **66**, 081302(R) (2002)
33. A. Laucht, M. Kaniber, A. Mohtashami, N. Hauke, M. Bichler, J.J. Finley, Phys. Rev. B **81**, 241302(R) (2010)
34. D. Elvira, R. Hostein, B. Fain, L. Moniello, A. Michon, G. Beaudoin, R. Braive, I. Robert-Philip, I. Abram, I. Sagnes, A. Beveratos, Phys. Rev. B **84**, 195302 (2011)
35. J. Suffczynski, A. Dousse, K. Gauthron, A. Lemaître, I. Sagnes, L. Lanco, J. Bloch, P. Voisin, P. Senellart, Phys. Rev. Lett. **103**, 027401 (2009)
36. M. Winger, T. Volz, G. Tarel, S. Portolan, A. Badolato, K.J. Hennessy, E.L. Hu, A. Beveratos, J. Finley, V. Savona, A. Imamoglu, Phys. Rev. Lett. **103**, 207403 (2009)
37. A. Predojevic, M. Jezek, T. Huber, H. Jayakumar, T. Kauten, G.S. Solomon, R. Filip, G. Weihs, Opt. Express **22**, 4789, (2014)
38. W.L. Barnes, G. Björk, J.-M. Gérard, P. Jonsson, J.A.E. Wasey, P.T. Worthing, V. Zwiller, Eur. Phys. J. D **18**, 197 (2002)
39. J.-M. Gérard, B. Sermage, B. Gayral, B. Legrand, E. Costard, V. Thierry-Mieg, Phys. Rev. Lett. **81**, 1110 (1998)
40. E. Moreau, I. Robert-Philip, J.-M. Gérard, I. Abram, L. Ferlazzo, V. Thierry-Mieg, Appl. Phys. Lett. **79**, 2865 (2001)
41. M. Pelton, C. Santori, J. Vuckovic, B. Zhang, G.S. Solomon, J. Plant, Y. Yamamoto, Phys. Rev. Lett. **89**, 233602 (2002)
42. W.-H. Chang, W.-Y. Chen, H.-S. Chang, T.-P. Hsieh, J.-I. Chyi, T.-M. Hsu, Phys. Rev. Lett. **96**, 117401 (2006)
43. S. Strauf, N.G. Stoltz, M.T. Rakher, L.A. Coldren, P.M. Petroff, D. Bouwmeester, Nat. Photon. **1**, 704 (2007)
44. A. Kiraz, P. Michler, C. Becher, B. Gayral, A. Imamoglu, L. Zhang, E. Hu, W.V. Schoenfeld, P.M. Petroff, Appl. Phys. Lett. **78**, 3932 (2001)
45. A. Högele, S. Seidl, M. Kroner, K. Karrai, R.J. Warburton, B.D. Gerardot, P.M. Petroff, Phys. Rev. Lett. **93**, 217401 (2004)
46. D. Haft, C. Schulhauser, A.Q. Govorov, R.J. Warburton, K. Karrai, J.M. Garcia, W. Schoedfeld, P.M. Petroff, Physica E **13**, 165 (2002)
47. S. Seidl, M. Kroner, A. Högele, K. Karrai, R.J. Warburton, A. Badolato, P.M. Petroff, Appl. Phys. Lett. **88**, 203113 (2006)
48. A. Faraon, D. Englund, D. Bulla, B. Luther-Davies, B.J. Eggleton, N. Stoltz, P. Petroff, J. Vuckovic, Appl. Phys. Lett. **92**, 043123 (2008)
49. S. Mosor, J. Hendrickson, B.C. Richards, J. Sweet, G. Khitrova, H.M. Gibbs, T. Yoshie, A. Scherer, O.B. Shchekin, D.G. Deppe, Appl. Phys. Lett. **87**, 141105 (2005)
50. A. Badolato, K. Hennessy, M. Atatüre, J. Dreiser, P.M. Petroff, A. Imamoglu, Science **308**, 1158 (2005)

51. A. Dousse, L. Lanco, J. Suffczynski, E. Semenova, A. Miard, A. Lemaître, I. Sagnes, C. Roblin, J. Bloch, P. Senellart, Phys. Rev. Lett. **101**, 267404 (2008)
52. T. Lund-Hansen, S. Stobbe, B. Julsgaard, H. Thyrrestrup, T. Sünner, M. Kamp, A. Forchel, P. Lodahl, Phys. Rev. Lett. **101**, 113903 (2008)
53. I. Friedler, P. Lalanne, J.-P. Hugonin, J. Claudon, J.-M. Gérard, A. Beveratos, I. Robert-Philip, Opt. Lett. **33**, 2635 (2008)
54. J. Claudon, J. Bleuse, N.S. Malik, M. Bazin, P. Jaffrennou, N. Gregersen, C. Sauvan, P. Lalanne, J.-M. Gérard, Nat. Photon. **4**, 174 (2010)
55. M.E. Reimer, G. Bulgarini, N. Akopian, M. Hocevar, M.B. Bavinck, M.A. Verheijen, E.P.A.M. Bakkers, L.P. Kouwenhoven, V. Zwiller, Nat. Commun. **3**, 737 (2012)
56. M. Munsch, N.S. Malik, E. Dupuy, A. Delga, J. Bleuse, J.M. Gérard, J. Claudon, N. Gregersen, J. Moerk, Phys. Rev. Lett. **110**, 177402 (2013)
57. M. Munsch, N.S. Malik, E. Dupuy, A. Delga, J. Bleuse, J.M. Gérard, J. Claudon, N. Gregersen, J. Moerk, Phys. Rev. Lett. **111**, 239902(E) (2013)
58. I. Friedler, C. Sauvan, J.P. Hugonin, P. Lalanne, J. Claudon, J.M. Gérard, Opt. Express **17**, 2095 (2009)
59. M. Munsch, J. Claudon, J. Bleuse, N.S. Malik, E. Dupuy, J.-M. Gérard, Y. Chen, N. Gregersen, J. Mork, Phys. Rev. Lett. **108**, 077405 (2012)
60. B.R. Mollow, Phys. Rev. **188**, 1969 (1969)
61. F.Y. Wu, R.E. Grove, S. Ezekiel, Phys. Rev. Lett. **35**, 1426 (1975)
62. A.N. Vamivakas, Y. Zhao, C.-Y. Lu, M. Atature, Nat. Phys. **5**, 198 (2009)
63. S. Ates, S.M. Ulrich, S. Reitzenstein, A. Löffler, A. Forchel, P. Michler, Phys. Rev. Lett. **103**, 167402 (2009)
64. A. Muller, E.B. Flagg, P. Bianucci, X.Y. Wang, D.G. Deppe, W. Ma, J. Zhang, G.J. Salamo, M. Xiao, C.K. Shih, Phys. Rev. Lett. **99**, 187402 (2007)
65. E.B. Flagg, A. Muller, J.W. Robertson, S. Founta, D.G. Deppe, M. Xiao, W. Ma, G.J. Salamo, C.K. Shih, Nat. Phys. **5**, 203 (2009)
66. A. Ulhaq, S. Weiler, S.M. Ulrich, R. Rossbach, M. Jetter, P. Michler, Nat. Photon. **6**, 238 (2012)
67. A. Faraon, I. Fushman, D. Englund, N. Stoltz, P. Petroff, J. Vuckovic, Nat. Phys. **4**, 859 (2008)
68. A. Reinhard, T. Volz, M. Winger, A. Badolato, K.J. Hennessy, E.L. Hu, A. Imamoglu, Nat. Photon. **6**, 93 (2012)
69. Z. Yuan, B. Kardynal, R.M. Stevenson, A.J. Shields, C. Lobo, K. Cooper, N.S. Beattie, D.A. Ritchie, M. Pepper, Science **295**, 102 (2002)
70. D.J.P. Ellis, A.J. Bennett, S.J. Dewhurst, C.A. Nicoll, D.A. Ritchie, A.J. Shields, New J. Phys. **10**, 043035 (2008)
71. T. Heindel, C. Schneider, M. Lermer, S.H. Kwon, T. Braun, S. Reitzenstein, S. Höfling, M. Kamp, A. Forchel, Appl. Phys. Lett. **96**, 011107 (2010)
72. A.K. Nowak, S.L. Portalupi, V. Giesz, O. Gazzano, C. Dal Savio, P.-F. Braun, K. Karrai, C. Arnold, L. Lanco, I. Sagnes, A. Lemaître, P. Senellart, Nat. Commun. **5**, 3240 (2014)
73. M.B. Ward, T. Farrow, P. See, Z.L. Yuan, O.Z. Karimov, A.J. Bennett, A.J. Shields, P. Atkinson, K. Cooper, D.A. Ritchie, Appl. Phys. Lett. **90**, 063512 (2007)
74. T. Miyazawa, T. Nakaoka, T. Usuki, Y. Arakawa, K. Takemoto, S. Hirose, S. Okumura, M. Takatsu, N. Yokoyama, Appl. Phys. Lett. **92**, 161104 (2008)
75. M.B. Ward, O.Z. Karimov, D.C. Unitt, Z.L. Yuan, P. See, D.G. Gevaux, A.J. Shields, P. Atkinson, D.A. Ritchie, Appl. Phys. Lett. **86**, 201111 (2005)
76. B. Alloing, C. Zinoni, V. Zwiller, L.H. Li, C. Monat, M. Gobet, G. Buchs, A. Fiore, E. Pelucchi, E. Kapon, Appl. Phys. Lett. **86**, 101908 (2005)
77. C. Zinoni, B. Alloing, C. Monat, V. Zwiller, L.H. Li, A. Fiore, L. Lunghi, A. Gerardino, H. de Riedmatten, H. Zbinden, N. Gisin, Appl. Phys. Lett. **88**, 131102 (2006)
78. N.I. Cade, H. Gotoh, H. Kamada, H. Nakano, S. Anantathanasarn, R. Nötzel, Appl. Phys. Lett. **89**, 181113 (2006)
79. M.D. Birowosuto, H. Sumikura, S. Matsuo, H. Taniyama, P.J. van Veldhoven, R. Nötzel, M. Notomi, Sci. Rep. **2**, 321 (2012)
80. K. Takemoto, Y. Sakuma, S. Hirose, T. Usuki, N. Yokoyama, Jpn J. Appl. Phys. **43**, L349 (2004)
81. T. Miyazawa, K. Takemoto, Y. Sakuma, S. Hirose, T. Usuki, N. Yokoyama, M. Takatsu, Y. Arakawa, Jpn J. Appl. Phys. **44**, L620 (2005)
82. M.T. Rakher, L. Ma, O. Slattery, X. Tang, K. Srinivasan, Nat. Photon. **4**, 786 (2010)
83. S. Zaske, A. Lenhard, C.A. Kessler, J. Kettler, C. Hepp, C. Arend, R. Albrecht, W.-M. Schulz, M. Jetter, P. Michler, C. Becher, Phys. Rev. Lett. **109**, 147404 (2012)
84. J.S. Pelc, L. Yu, K. De Greve, P.L. McMahon, C.M. Natarajan, V. Esfandyarpour, S. Maier, C. Schneider, M. Kamp, S. Höfling, R.H. Hadfield, A. Forchel, Y. Yamamoto, M.M. Fejer, Opt. Express **20**, 27510 (2012)
85. S. Ates, I. Agha, A. Gulinatti, I. Rech, M.T. Rakher, A. Badolato, K. Srinivasan, Phys. Rev. Lett. **109**, 147405 (2012)
86. M.W. McCutcheon, D.E. Chang, Y. Zhang, M.D. Lukin, M. Loncar, Opt. Express **17**, 22689 (2009)
87. A. Pe'er, B. Dayan, A.A. Friesem, Y. Silberberg, Phys. Rev. Lett. **94**, 073601 (2005)
88. P. Kolchin, C. Belthangady, S. Du, G.Y. Yin, S.E. Harris, Phys. Rev. Lett. **101**, 103601 (2008)
89. H.P. Specht, J. Bochmann, M. Mücke1, B. Weber, E. Figueroa, D.L. Moehring, G. Rempe, Nat. Photon. **3**, 469 (2009)
90. P. Michler, *Single Semiconductor Quantum Dots* (Springer, 2009)
91. C. Kammerer, C. Voisin, G. Cassabois, C. Delalande, Ph. Roussignol, F. Klopf, J.P. Reithmaier, A. Forchel, J.-M. Gérard, Phys. Rev. B **66**, 041306 (2002)
92. I. Favero, A. Berthelot, G. Cassabois, C. Voisin, C. Delalande, Ph. Roussignol, R. Ferreira, J.-M. Gérard, Phys. Rev. B **75**, 073308 (2007)
93. C. Santori, D. Fattal, J. Vuckovic, G.S. Solomon, Y. Yamamoto, Nature **419**, 594 (2002)
94. C.K. Hong, Z.Y. Ou, L. Mandel, Phys. Rev. Lett. **59**, 2044 (1987)
95. S. Varoutsis, S. Laurent, P. Kramper, A. Lemaître, I. Sagnes, I. Robert-Philip, I. Abram, Phys. Rev. B **72**, 041303(R) (2005)
96. A. Bennett, D. Unitt, A. Shields, P. Atkinson, D. Ritchie, Opt. Express **13**, 7772 (2005)
97. S. Laurent, S. Varoutsis, L. Le Gratiet, A. Lemaître, I. Sagnes, F. Raineri, J.A. Levenson, I. Robert-Philip, I. Abram, Appl. Phys. Lett. **87**, 163107 (2005)
98. O. Gazzano, S. Michaelis de Vasconcellos, C. Arnold, A.K. Nowak, E. Galopin, I. Sagnes, L. Lanco, A. Lemaître, P. Senellart, Nat. Commun. **4**, 1425 (2013)

99. S. Weiler, D. Stojanovic, S.M. Ulrich, M. Jetter, P. Michler, Phys. Rev. B **87**, 241302(R) (2013)
100. Y.-M. He, Y. He, Y.-J. Wei, D. Wu, M. Atatüre, C. Schneider, S. Höffling, M. Kamp, C.-Y. Lu, J.-W. Pan, Nat. Nanotechnol. **8**, 213 (2013)
101. L. Monniello, A. Reigue, R. Hostein, A. Lemaître, A. Martinez, R. Grousson, V. Voliotis, Phys. Rev. B **90**, 041303(R) (2014)
102. H.S. Nguyen, G. Sallen, C. Voisin, P. Roussignol, C. Diederichs, G. Cassabois, Appl. Phy. Lett. **99**, 261904 (2011)
103. C. Matthiesen, A.N. Vamvakas, M. Atatüre, Phys. Rev. Lett. **108**, 093602 (2012)
104. R. Proux, M. Maragkou, E. Baudin, C. Voisin, P. Roussignol, C. Diederichs, `arXiv:1404.1244` (2014)
105. A.J. Bennett, R.B. Patel, A.J. Shields, K. Cooper, P. Atkinson, C.A. Nicoll, D.A. Ritchie, Appl. Phys. Lett. **92**, 193503 (2008)
106. A. Aspect, P. Grangier, G. Roger, Phys. Rev. Lett. **49**, 91 (1982)
107. Z.Y. Ou, L. Mandel, Phys. Rev. Lett. **61**, 50 (1988)
108. Y.H. Shih, C.O. Alley, Phys. Rev. Lett. **61**, 2921 (1988)
109. D. Fattal, K. Inoue, J. Vuckovic, C. Santori, G.S. Solomon, Y. Yamamoto, Phys. Rev. Lett. **92**, 037904 (2004)
110. M. Larque, A. Beveratos, I. Robert-Philip, Eur. Phys. J. D **47**, 119 (2008)
111. J.D. Franson, Phys. Rev. Lett. **62**, 2205 (1989)
112. I. Marcikic, H. de Riedmatten, W. Tittel, V. Scarani, H. Zbinden, N. Gisin, Phys. Rev. A **66**, 062308 (2002)
113. W. Tittel, J. Brendel, N. Gisin, H. Zbinden, Phys. Rev. A **59**, 4150 (1999)
114. A.J. Bennett, D.G. Gevaux, Z.L. Yuan, A.J. Shields, P. Atkinson, D.A. Ritchie, Phys. Rev. A **77**, 023803 (2008)
115. C. Simon, J.-P. Poizat, Phys. Rev. Lett. **94**, 030502 (2005)
116. P.K. Pathak, S. Hughes, Phys. Rev. B **83**, 245301 (2011)
117. H. Jayakumar, A. Predojević, T. Kauten, T. Huber, G.S. Solomon, G. Weihs, Nat. Commun. **5**, 4251 (2014)
118. R.M. Stevenson, R.J. Young, P. See, D.G. Gevaux, K. Cooper, P. Atkinson, I. Farrer, D.A. Ritchie, A.J. Shields, Phys. Rev. B **73**, 033306 (2006)
119. K. Kowalik, O. Krebs, A. Lemaître, S. Laurent, P. Senellart, P. Voisin, J.A. Gaj, Appl. Phys. Lett. **86**, 041907 (2005)
120. B.D. Gerardot, S. Seidl, P.A. Dalgarno, R.J. Warburton, D. Granados, J.M. Garcia, K. Kowalik, O. Krebs, K. Karrai, A. Badolato, P.M. Petroff, Appl. Phys. Lett. **90**, 041101 (2007)
121. A.J. Bennett, M.A. Pooley, R.M. Stevenson, M.B. Ward, R.B. Patel, A. Boyer de la Giroday, N. Sköld, I. Farrer, C.A. Nicoll, D.A. Ritchie, A.J. Shields, Nat. Phys. **6**, 947 (2010)
122. D.J.P. Ellis, R.M. Stevenson, R.J. Young, A.J. Shields, P. Atkinson, D.A. Ritchie, Appl. Phys. Lett. **90**, 011907 (2007)
123. R.J. Young, R.M. Stevenson, A.J. Shields, P. Atkinson, K. Cooper, D.A. Ritchie, K.M. Groom, A.I. Tartakovskii, M.S. Skolnick, Phys. Rev. B **72**, 113305 (2005)
124. R. Trotta, E. Zallo, C. Ortix, P. Atkinson, J.D. Plumhof, J. van den Brink, A. Rastelli, O.G. Schmidt, Phys. Rev. Lett. **109**, 147401 (2012)
125. M. Larque, I. Robert-Philip, A. Beveratos, Phys. Rev. A **77**, 42118 (2008)
126. R. Johne, N.A. Gippius, G. Pavlovic, D.D. Solnyshkov, I.A. Shelykh, G. Malpuech, Phys. Rev. Lett. **100**, 240404 (2008)
127. N. Akopian, N.H. Lindner, E. Poem, Y. Berlatzky, J. Avron, D. Gershoni, B.D. Gerardot, P.M. Petroff, Phys. Rev. Lett. **96**, 130501 (2006)
128. R.M. Stevenson, R.J. Young, P. Atkinson, K. Cooper, D.A. Ritchie, A.J. Shields, Nature **439**, 179 (2006)
129. M. Gahli, K. Ohtani, Y. Ohno, H. Ohno, Nat. Commun. **3**, 661 (2012)
130. A. Muller, W. Fang, J. Lawall, G.S. Solomon, Phys. Rev. Lett. **103**, 217402 (2009)
131. A. Dousse, J. Suffczynski, A. Beveratos, O. Krebs, A. Lemaître, I. Sagnes, J. Bloch, P. Voisin, P. Senellart, Nature **466**, 217 (2010)
132. R.M. Stevenson, A.J. Hudson, Robert A.J. Bennett, J. Young, C.A. Nicoll, D.A. Ritchie, A.J. Shields, Phys. Rev. Lett. **101**, 170501 (2008)
133. R.J. Young, R.M. Stevenson, A.J. Hudson, C.A. Nicoll, D.A. Ritchie, A.J. Shields, Phys. Rev. Lett. **102**, 030406 (2009)
134. C.L. Salter, R.M. Stevenson, I. Farrer, C.A. Nicoll, D.A. Ritchie, A.J. Shields, Nature **465**, 594 (2010)
135. A.J. Hudson, R.M. Stevenson, A.J. Bennett, R.J. Young, C.A. Nicoll, P. Atkinson, K. Cooper, D.A. Ritchie, A.J. Shields, Phys. Rev. Lett. **99**, 266802 (2007)
136. M. Larque, T.J. Karle, I. Robert-Philip, A. Beveratos, New J. Phys. **11**, 33022 (2009)
137. I.S. Maksymov, M. Besbes, J.-P. Hugonin, J. Yang, A. Beveratos, I. Sagnes, I. Robert-Philip, P. Lalanne, Phys. Rev. Lett. **105**, 180502 (2010)
138. R.M. Stevenson, C.L. Salter, J. Nilsson, A.J. Bennett, M.B. Ward, I. Farrer, D.A. Ritchie, A.J. Shields, Phys. Rev. Lett. **108**, 040503 (2012)
139. M. Müller, S. Bounouar, K.D. Jöns, M. Gläss, P. Michler, Nat. Photon. **8**, 224 (2014)
140. D. Fattal, E. Diamanti, K. Inoue, Y. Yamamoto, Phys. Rev. Lett. **92**, 037904 (2004)
141. E. Waks, K. Inoue, C. Santori, D. Fattal, J. Vuckovic, G.S. Solomon, Y. Yamamoto, Nature **420**, 762 (2002)
142. P.M. Intallura, M.B. Ward, O.Z. Karimov, Z.L. Yuan, P. See, A.J. Shields, P. Atkinson, D.A. Ritchie, Appl. Phys. Lett. **91**, 161103 (2007)
143. T. Heindel, C.A. Kessler, M. Rau, C. Schneider, M. Fürst, F. Hargart, W.-M. Schulz, M. Eichfelder, R. Rossbach, S. Nauerth, M. Lermer, H. Weier, M. Jetter, M. Kamp, S. Reitzenstein, S. Höfling, P. Michler, H. Weinfurter, A. Forchel, New J. Phys. **14**, 083001 (2012)
144. K. Takemoto, Y. Nambu, T. Miyazawa, K. Wakui, S. Hirose, T. Usuki, M. Takatsu, N. Yokoyama, K. Yoshino, A. Tomita, S. Yorozu, Y. Sakuma, Y. Arakawa, Appl. Phys. Express **3**, 092802 (2010)

145. M. Scholz, T. Aichele, S. Ramelow, O. Benson, Phys. Rev. Lett. **96**, 180501 (2006)
146. M.A. Pooley, D.J.P. Ellis, R.B. Patel, A.J. Bennett, K.H.A. Chan, I. Farrer, D.A. Ritchie, A.J. Shields, Appl. Phys. Lett. **100**, 211103 (2012)
147. O. Gazzano, M.P. Almeida, A.K. Nowak, S.L. Portalupi, A. Lemaître, I. Sagnes, A.G. White, P. Senellart, Phys. Rev. Lett. **110**, 250501 (2013)
148. N. Akopian, L. Wang, A. Rastelli, O.G. Schmidt, V. Zwiller, Nat. Photon. **5**, 230 (2011)
149. G. Reithmaier, S. Lichtmannecker, T. Reichert, P. Hasch, K. Müller, M. Bichler, R. Gross, J.J. Finley, Sci. Rep. **3**, 1901 (2013)
150. C. Matthiesen, M. Geller, C.H.H. Schulte, C. Le Gall, J. Hansom, Z. Li, M. Hugues, E. Clarke, M. Atatüre, Nat. Commun. **4**, 1600 (2013)
151. N. Koguchi, S. Takahashi, T. Chikyow, J. Cryst. Growth **111**, 688 (1991)
152. P. Tighineanu, R. Daveau, E.H. Lee, J.D. Song, S. Stobbe, P. Lodahl, Phys. Rev. B **88**, 155320 (2013)
153. G. Sallen, B. Urbaszek, M.M. Glazov, E.L. Ivchenko, T. Kuroda, T. Mano, S. Kunz, M. Abbarchi, K. Sakoda, D. Lagarde, A. Balocchi, X. Marie, T. Amand, Phys. Rev. Lett. **107**, 166604 (2011)
154. T. Kuroda, T. Mano, N. Ha, H. Nakajima, H. Kumano, B. Urbaszek, M. Jo, M. Abbarchi, Y. Sakuma, K. Sakoda, I. Suemune, X. Marie, T. Amand, Phys. Phys. B **88**, 041306(R) (2013)
155. X. Liu, N. Ha, H. Nakajima, T. Mano, T. Kuroda, B. Urbaszek, H. Kumano, I. Suemune, Y. Sakuma, K. Sakoda, Phys. Rev. B **90**, 081301(R) (2014)
156. E.B. Flagg, A. Muller, S.V. Polyakov, A. Ling, A. Migdall, G.S. Solomon, Phys. Rev. Lett. **104**, 137401 (2010)
157. R.B. Patel, A.J. Bennett, I. Farrer, C.A. Nicoll, D.A. Ritchie, A.J. Shields, Nat. Photon. **4**, 632 (2010)
158. M.H. Baier, E. Pelucchi, E. Kapon, S. Varoutsis, M. Gallart, I. Robert-Philip, I. Abram, Appl. Phys. Lett. **84**, 648 (2004)
159. K.D. Jöns, P. Atkinson, M. Müller, M. Heldmaier, S.M. Ulrich, O.G. Schmidt, P. Michler, Nano Lett. **13**, 126 (2013)
160. H.Z. Song, T. Usuki, S. Hirose, K. Takemoto, Y. Nakata, N. Yokoyama, Y. Sakuma, Appl. Phys. Lett. **86**, 113118 (2005)
161. G. Juska, V. Dimastrodonato, L.O. Mereni, A. Gocalinska, E. Pelucchi, Nat. Photon. **7**, 527 (2013)
162. M.T. Bjork, C. Thelander, A.E. Hansen, L.E. Jensen, M.W. Larsson, L.R. Wallenberg, L. Samuelson, Nano Lett. **4**, 1621 (2004)
163. G. Bulgarini, M.E. Reimer, M.B. Bavinck, K.D. Jöns, D. Dalacu, P.J. Poole, E.P.A.M. Bakkers, V. Zwiller, Nano Lett. **14**, 4102 (2014)
164. M.A.M. Versteegh, M.E. Reimer, K.D. Jöns, D. Dalacu, P.J. Poole, A. Gulinatti, A. Giudice, V. Zwiller, Nat. Commun. **5**, 5298 (2014)
165. D. Press, K. De Greve, P.L. McMahon, T.D. Ladd, B. Friess, C. Schneider, M. Kamp, S. Höfling, A. Forchel, Y. Yamamoto, Nat. Photon. **4**, 367 (2010)
166. M. Atatüre, J. Dreiser, A. Badolato, A. Högele, K. Karrai, A. Imamoglu, Science **312**, 551 (2006)
167. B.D. Gerardot, D. Brunner, P.A. Dalgarno, P. Ohberg, S. Seidl, M. Kroner, K. Karrai, N.G. Stoltz, P.M. Petroff, R.J. Warburton, Nature **451**, 441 (2008)
168. J. Berezovsky, M.H. Mikkelsen, N.G. Stoltz, L.A. Coldren, D.D. Awschalom, Science **320**, 349 (2008)
169. D. Press, T.D. Ladd, B. Zhang, Y. Yamamoto, Nature **456**, 218 (2008)
170. D. Kim, S.G. Carter, A. Greilich, A.S. Bracker, D. Gammon, Nat. Phys. **7**, 223 (2011)
171. W.B. Gao, P. Fallahi, E. Togan, J. Miguel-Sanchez, A. Imamoglu, Nature **491**, 426 (2012)
172. W.B. Gao, P. Fallahi, E. Togan, A. Delteil, Y.S. Chin, J. Miguel-Sanchez, A. Imamoglu, Nat. Commun. **4**, 2744 (2013)
173. I.J. Luxmoore, N.A. Wasley, A.J. Ramsay, A.C.T. Thijssen, R. Oulton, M. Hugues, S. Kasture, V.G. Achanta, A.M. Fox, M.S. Skolnick, Phys. Rev. Lett. **110**, 037402 (2013)
174. R.J. Warburton, Nat. Mater. **12**, 486 (2012)
175. B. Urbaszek, X. Marie, T. Amand, O. Krebs, P. Voisin, P. Maletinsky, A. Hogele, A. Imamoglu, Rev. Mod. Phys. **85**, 79 (2013)